Vehicular Trajectory Optimization for Cooperative Collision Avoidance at High Speeds

Juan-Bautista Tomas-Gabarron, Esteban Egea-Lopez, and Joan Garcia-Haro, *Member, IEEE*

***Abstract*—Traffic safety is a key aspect in new-generation intelligent transportation systems. Among other areas, an active field of research is cooperative collision avoidance, where vehicles cooperatively calculate trajectories under tight time constraints to avoid colliding under specific road-traffic domains (overtaking, intersections, etc.). In this paper, we particularly analyze the problem of collision avoidance in scenarios in which high-speed vehicles need to generate evasive maneuvers within very short time intervals to avoid or at least mitigate a hypothetical (multiple) collision. We pose this as a multiobjective optimization problem and simplify it by considering only lateral motion for the optimization process, thus having to solve a 1-D trajectory generation problem. The routes of vehicles are optimized according to a weighted aggregation functional that: 1) maximizes the lateral distances between vehicle–vehicle and vehicle–obstacle pairs at the time of overcoming the obstacles; 2) minimizes the lateral speeds at the end of the path; and 3) minimizes the instantaneous lateral acceleration (inertia) along the maneuver. In addition, we compute trajectories by following an optimization strategy that divides the problem into a set of independent subproblems, which are optimized in parallel by using a gradient-descent-based methodology. From this set of solutions, the most suitable option, according to our selected criteria, is chosen. Results show the utility of our approach and its flexibility to compute evasive trajectories adapted to different requirements. Additionally, a simulation of the mechanical response of the vehicles during the evasive maneuvers is conducted.**

***Index Terms*—Cooperative collision avoidance (CCA), optimum control, optimum maneuvering, road accidents, VANET, vehicle safety.**

NOMENCLATURE

L	Number of vehicles.
M	Number of intermediate obstacles ($M \geq 0$).
N	Discretization factor.
O	Number of lanes.
W_l	Lane width [m].
W_i	Width of the internal edge of the road [m].
W_e	Width of the external edge of the road [m].
W	Total road width: $O \times W_l + W_i + W_e$ [m].
j	Subindex to refer to vehicle $j \in \{1, \ldots, L\}$.
β	Subindex to refer to obstacle ($\beta \in \{1, \ldots, M+2\}$), or gap ($\beta \in \{1, \ldots, M+1\}$).
k	Discrete instant for each trajectory, $k \in \{1, \ldots, N\}$.
t_f	Maneuverability time interval [s].
v_I	Longitudinal speed [m/s].
l	Distance to obstacles [m].
Δt	Discretized time lapse $\Delta t = t_f/N$.
$x_j(t)$	Lateral position of vehicle j [m] at time t.
$x_j(k)$	Lateral position of vehicle j [m] at discrete instant k.
w_j	Width of vehicle j [m].
$v_j(t)$	Lateral speed of vehicle j [m/s] at time t.
$a_j(t)$	Lateral acceleration of vehicle j [m/s^2] at time t.
z_β	Position of obstacle β [m].
o_β	Width of obstacle β [m].
X_{0j}	Initial lateral position of vehicle j [m].
V_{0j}	Initial lateral speed of vehicle j [m/s].
A_{0j}	Initial lateral acceleration of vehicle j [m/s^2].
v_I	Longitudinal speed [m/s].
$c_j(v_I)$	Function to calculate the maximum lateral acceleration (from the longitudinal speed) [m/s^2] for vehicle j.
$\gamma_j(t)$	Steering angle of vehicle j at time t.
θ_x	Weighting factor of f_x, $f_{m,x}$.
θ_v	Weighting factor of f_v.
θ_a	Weighting factor of f_a.
$R_{L,M+1}$	Number of *weak compositions* of L vehicles into $M+1$ gaps.
m	Index to represent the mth solution of the *weak* $(M+1)$*-composition of* L.
$J_{L,M}^{(q)}$	Subfunctional for the combination q.
$\overline{J_{L,M}}$	Performance cost that minimizes the set of combinations.
$\sigma^2_{m,\mathrm{dist}}$	Squared sum of lateral distances for combination m.
$G_{m,\beta}^{(L,M)}$	Number of vehicles in gap β for the combination m (distribution of L vehicles into $M+1$ gaps).
$\Xi_{m,l}^{(L,M)}$	Number of accumulated vehicles for the first l gaps in combination m (for the distribution of L vehicles into $M+1$ gaps).
$\phi_{m,\beta}(t)$	Squared sum of lateral distances for vehicles between obstacles in gap β of combination m.
δ	Time interval taken by the algorithm to compute trajectories.
ϵ	Longitudinal distance error obtained for the mapped path.

Manuscript received October 30, 2012; revised April 6, 2013 and June 13, 2013; accepted June 16, 2013. This work was supported by Project Spanish Ministry of Economy and Competitiveness (MINECO)/European Regional Development Fund (FEDER) under Grant TEC2010-21405-C02-02/TCM (CALM). It was also developed in the framework of *Programa de Ayudas a Grupos de Excelencia de la Región de Murcia, Fundación Séneca'*. The work of J. B. Tomas-Gabarron was supported by the Spanish MINECO through a University Professorship Formation (FPU) Predoctoral Fellowship under Grant REF AP2008-02244. The Associate Editor for this paper was A. Amditis.

J.-B. Tomas-Gabarron, E. Egea-Lopez, and J. Garcia-Haro are with the Department of Information Technologies and Communications, Technical University of Cartagena (UPCT), 30202 Cartagena, Spain.

Color versions of one or more of the figures in this paper are available online at http://ieeexplore.ieee.org.

Digital Object Identifier 10.1109/TITS.2013.2270009

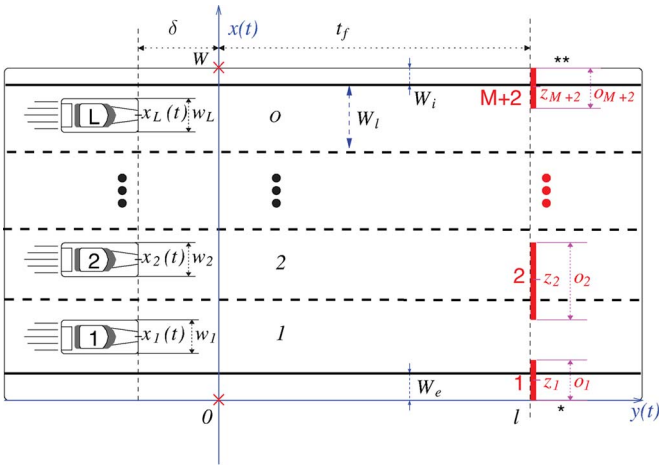

Fig. 1. General scenario under analysis.

I. Introduction

ROAD SAFETY applications for vehicular networks are now the focus of numerous research groups around the world [1], [2]. More importantly, special attention is given to applications aimed at solving safety issues in specific situations. That is the case, for example, of cooperative collision avoidance (CCA) applications, which allow interconnected vehicles to calculate trajectories in particular domains of the road traffic, such as intersections [3], overtakes [4], or general obstacle/rear-end collision avoidance [5], [6].

Particularly, in this paper, we focus on the generation of optimum trajectories for autonomous vehicles under critical obstacle avoidance circumstances: specifically, for those situations in which high-speed vehicles need to cooperatively calculate evasive maneuvers within short intervals of time (around 1 s) to avoid collisions between them and with objects appearing along the direction of transit (see Fig. 1). We assume that the whole process can be tentatively classified into the following four consecutive stages:

1) Obstacle detection and risk estimation.
2) Computation of preview trajectories.
3) Dissemination of information for the agreement.[1]
4) Tracking of the trajectories (execution of maneuvers).

In this particular study, we focus exclusively on the second stage. After the delay associated to the trajectory generation phase, vehicles will start tracking the given paths simultaneously. In addition, although we do not consider in detail the dynamic effects of the tracking phase, in this paper, we check that the preview trajectories can be effectively tracked by using a realistic vehicle mechanics simulator (CarSim) [7]. Specific details on the other stages are out of the focus of the present research and left for a future work.

We model the aforementioned scenario as a multiobjective optimization problem (MOP), for which we assume that trajectories are exclusively determined by the lateral vehicular accelerations, which we have to calculate according to the corresponding optimization of the proposed performance cost function, considering the longitudinal speed constant during the maneuver. This approach allows us to consider a 1-D trajectory generation problem that decouples the effects of the longitudinal and lateral mobility, thus reducing the complexity of the calculation process. These assumptions are justified under certain conditions of mobility, as discussed in Section V and in the Appendix. We also consider three different weighted criteria to shape trajectories according to specific mobility aspects. First, from the point of view of safety, vehicles should keep a maximum separation between them and the obstacles at the instant they reach the obstacles' positions. Second, it is also important to control (minimize) the lateral speed at the moment of passing through the obstacles, so that hypothetical lateral collisions with other vehicles and/or crash barriers can be avoided after obstacles are left behind. Finally, inertial movement (accelerations) during the evolution of the maneuvers should be minimized for an improved sense of comfort and, more importantly, for a higher degree of stability of the car body during the steering maneuver. In addition, the resolution strategy treats the trajectory generation scheme as a set of separate optimization problems, every one of which deals with the optimization of trajectories, as determined by how vehicles can distribute their paths through the free gaps at the laterals of the obstacles. This will be explained later in detail.

In summary, the goals of this paper are to describe the theoretical details of the trajectory generation algorithm, evaluate the influence and tradeoffs for the aforementioned three components of the performance cost functional, discuss the applicability of the algorithm given the time-demanding requisites of generic CCA applications, and assess the dynamic behavior of the vehicles while executing the trajectories under the CarSim mechanics simulator [7]. The main contributions are the formulation of the trajectory generation scheme as a 1-D path optimization problem by using a simplified yet robust vehicle kinematics model that is specially suitable for the specific conditions of the scenario evaluated. We additionally show that the assumptions made in this paper are actually consistent for situations in which vehicles need to cooperatively agree on a set of evasive actions within very short intervals of time (see the Appendix).

The rest of this paper is organized as follows. In Section II, relevant works on optimum trajectory generation for collision avoidance are presented. Section III introduces the optimization concepts used to analyze the problem at hand, as well as the specific method carried out to solve it. In Section IV, a characterization of the mathematical model applied to a vehicular scenario under critical circumstances is shown, in order to evaluate the performance of our proposal. Section V discusses the most important characteristics of the model and the results obtained in Section IV. The paper is finalized with the conclusions derived from the present research (see Section VI). One appendix is additionally included for the justification of the given model assumptions.

II. Related Work

Although there is already a considerable amount of studies regarding motion planning for collision avoidance in general

[1]In a real implementation, phases 2 and 3 might overlap, although we skip this consideration in this paper.

robots (see, for example, the pioneering studies in [8] and [9]), in the particular context of cooperative trajectory generation for high-speed automobiles, this has not been examined extensively until very recently. In this regard, the following three main approaches can be identified in the open literature: 1) collision avoidance by force fields (elastic bands), 2) maneuver selection by tree search/cell decomposition, and 3) path planning by optimum control.

The method of force fields is based on the assumption that collision-free paths are determined by a series of elastic bands that can be deformed through the influence of force fields (see, for example, the early works of [10] on motion planning for general robots and the work of [11], closer to our subject of study). The direction and intensity of this influence depend on the kinematic parameters of other neighboring elements (obstacles, vehicles, pedestrians, etc.), repelling the elastic band toward the free zones of the road. This method generally exhibits good performance for applications with real-time requirements [12] and scalability for use in general collision avoidance scenarios, such as intersection management [3], overtaking, and obstacle circumvention [4], [13], for example. However, it depends tightly on the initial configuration of the strings, possibly leading to local minima in the solution space that might correspond to trajectories unable to be tracked in practice if the inertial constraints are violated by the planned path [14], [15].

Tree search (also called cell decomposition [16]) treats the problem by selecting the appropriate maneuver out of a set of precomputed cooperative actions (braking, evasive steering, etc.) that are defined and rated for each vehicle by a loss function that penalizes constraints' violations [17]. This method discretizes the space of possible solutions during the interval $[0, t_f]$ at equally spaced time steps Δt when the maneuver must be executed [18], requiring, in general, highly demanding computation capabilities for potential real-time applicability [12] if fine-grained resolution is used (actually, by employing coarser discretization or pruning-precomputation methods [17], more acceptable processing delays, yet not for generic real-time purpose, can be obtained, at the expense of lower trajectory accuracy). However, in comparison with potential field approaches, a tree search may result in globally optimum maneuvers, even allowing extra trajectory shaping mechanisms for collision mitigation (if the crash is unavoidable), increased comfort (less inertial impact) and/or reduced gas consumption [14].

Path planning for obstacle avoidance by using optimum control consists, essentially, of the calculation of trajectories according to the optimization of some performance cost established beforehand [19]. Problems can be formulated as single-/multiobjective optimization, aimed at numerically obtaining trajectories whose shape can be adapted to different preestablished criteria, i.e., minimum time [20], minimum covered distance [21], minimum kinetic energy [22], maximized comfort [23], or a combination of those [24], while principally maximizing safety, by, for instance, increasing the distance between the vehicle and the obstacle and with the crash barriers [25]. Similar to the previous case, optimum control gives the decision-maker a great deal of flexibility for shaping trajectories according to arbitrary criteria, but suffers from a relatively high computational complexity, particularly for nonlinear optimization problems, that limits its functionality under real-time constraints. This counterproductive feature can be alleviated by decoupling dimensions in the solution space of the problem and, under certain assumptions, carry out a computationally less demanding optimization of the cost functional. In our proposal, corresponding to an optimum control approach, this is exactly what we do, namely, a reduction of the solution space to a 1-D trajectory generation problem, considering that, for sufficiently high longitudinal speeds, the steering angle while maneuvering can be neglected (in the optimization phase), so that the maneuverability time interval t_f can be kept fixed and focus only on the lateral mobility (see the Appendix). By doing so, it is possible to reduce the associated computational complexity and simultaneously obtain processing costs that can match tight time requisites (see Section IV), but under relatively rigid conditions of the scenario under evaluation (Section V). In addition, we take into consideration the optimization of different combinations of vehicular headings through obstacles, without the need for specifying all the multiple path branches that would have to be precomputed if tree search was applied, while obtaining more accurate trajectories. This feature makes it easy to benefit from parallel computing, such as in the tree search algorithm, with a much less number of combinations to process (see details in Section III-B).

III. Problem Statement and Formulation

Let us consider a scenario such as the one shown in Fig. 1, where a total of L vehicles (a maximum of one vehicle per lane) circulate on a 2-D planar road (O lanes with W_l m of width, external edge with W_e m of width, and internal edge with W_i m of width). Assume that vehicles have width and length dimensions and that their positions with respect to the given pair of axes are referenced according to the central front part of each one, that is, $\{[x_1(t), y_1(t)], \ldots, [x_L(t), y_L(t)]\}$ (see Fig. 1). For tractability of the problem, let us consider also that longitudinal speeds are constant and fixed to v_I m/s $\forall t \geq -\delta$ and that all vehicles keep the same longitudinal position at the initial instant[2] $t = -\delta$ s, that is, $y_j(-\delta) = -\delta \cdot v_I \quad \forall j \in \{1, \ldots, L\}$. Given that, at $t = -\delta$ s, a total of $M + 2$, 1-D obstacles are discovered $\delta \cdot v_I + l$ meters ahead, vehicles need δ s to process information and cooperatively agree on an optimum set of trajectories, which will be initiated synchronously by all of them after this first phase ends[3] (at $t = 0$ s) and will comprise a duration of t_f s. The complete process will thus cover a total of $t_m = \delta + t_f = \delta + l/v_I$ s from the moment the obstacles are first-time detected until vehicles reach the longitudinal position of these obstacles $y_j(t_f) = l$. Thus, we wish to determine the trajectories' evolution of the L vehicles during the time interval $[0, t_f]$ (assuming that, during the cooperative agreement phase, lateral components of mobility do not change) that can avoid

[2]We consider the initial instant to be $t = -\delta$ s to let the cooperative maneuvers begin at $t = 0$ s, for mathematical consistency with the integration indexes in the performance cost functions (see Section III-B).

[3]The specific approach by which the negotiation scheme takes place is out of the scope of this work. We will assume that, after δ s, the L vehicles start synchronously the execution of the previously determined maneuvers (at $t = 0$ s).

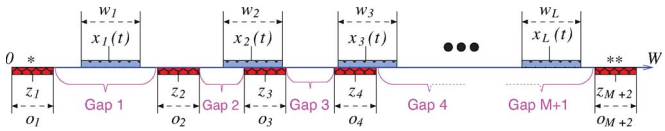

Fig. 2. x-axis projections of elements.

the collision with the obstacles, with each other and with the lateral crash barriers, while optimizing some other mobility parameters established beforehand.

Given the assumptions previously presented, we can restrict the problem to only governing the lateral mobility and model the lateral motion of vehicles with the usual laws of kinematics as

$$\begin{cases} \dot{x}_j(t) = v_j(t) \\ \dot{v}_j(t) = a_j(t) \end{cases} \qquad \forall j \in \{1, \ldots, L\}, \quad \forall t \in [0, t_f] \qquad (1)$$

where $x_j(t) \in \mathbb{R}$ defines the instantaneous lateral position of vehicle j according to axis x, $v_j(t) \in \mathbb{R}$ denotes the associated lateral speed of vehicle j, and $a_j(t) \in \mathbb{R}$ symbolizes the lateral acceleration of vehicle j. According to (1), the control domain variable that manages the mobility of each vehicle is the lateral acceleration $a_j(t)$.

Since our analysis reduces to the lateral motion of vehicles, we can perform a *projection* of the widths of vehicles and obstacles onto the x-axis, as shown in Fig. 2 (x-axis projection), where w_j corresponds to the width[4] of vehicle j, while z_k and o_k refer to the central position and the width of obstacle k, respectively. The idea is to find an admissible control history, in this case, the lateral accelerations $a_j(t)$, resulting in a set of 1-D trajectories $x_j(t)$, which minimizes a given performance metric or functional $J_{L,M}$ (see Section III-B). We will also assume that: 1) vehicles can only move within the width limits of the road $[0, W]$ (see Fig. 1); 2) the x-axis projections of vehicles cannot overlap on each other, which means that vehicular trajectories do not cross; 3) obstacles keep fixed and static, and their projections can be overlapped by the vehicles' projections during the lateral motion. Additionally, the controls are subject to further constraints, that is, there is a maximum admissible lateral acceleration. Statements 1), 2), and 3), as well as the constraints on the maximum allowable acceleration, are translated into state constraints as we will show. We consider the minimum number of obstacles to be two ($M = 0$), both located at the two ends of the laterals of the road (crash barriers), that is, symbols $(^*)$ and $(^{**})$, respectively, in Fig. 1.

As we discuss in detail later in Section III-B, the trajectory generation problem is divided into a set of optimization subproblems, each one regarding the optimization of a specific pass-through scheme associated to the particular path combination,[5] from the set of possibilities, that vehicles can choose to cross the obstacles (by turning through the free remaining gaps; see Fig. 3 for a given example). From this set of subproblems, we will select the most suitable solution, according to the particular performance criteria established by our algorithm (see Section III-B). First, we will introduce the state and control constraints that the vehicular dynamics in our model must obey. Second, we formulate the problem as a MOP. In the next subsections, we describe these steps in detail.

[4]The x-axis projection of the width of a generic vehicle j is assumed to be equal to w_j regardless of the orientation of its associated trajectory, since the variability of the width's projection would increase the complexity of the problem in the constraining relations [nonlinearity of inequalities (3), see Section III-A] and the expression of the performance metric. Moreover, since longitudinal speed v_I is much higher than lateral speed $v_j(t)$, this variability can be neglected.

[5]We will refer to this as combination or composition indistinctively throughout the paper.

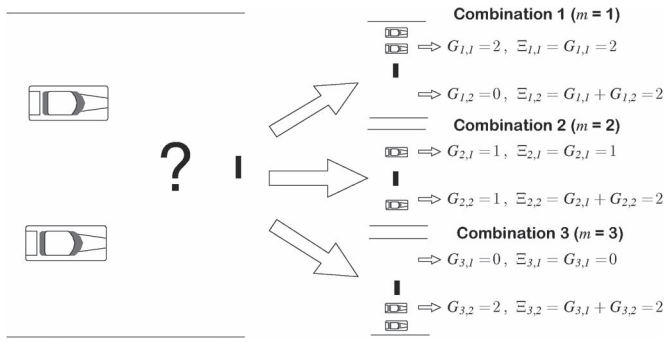

Fig. 3. Example of combination reordering for $M = 1$, $L = 2$. Each alternative is a *weak* $(M + 1)$*-composition of* L.

A. State Constraints

The state variables and the controls must adjust to the physical constraints of car motion. In this paper, we will introduce the following two main state restrictions:

1) **Lateral acceleration restrictions**. The absolute value of the lateral acceleration cannot take a value higher than the limit $c_j(v_I)$ m/s^2, where v_I is the constant longitudinal speed of all vehicles, and $c_j(\cdot) : \mathbb{R} \to \mathbb{R}$ is a function of the longitudinal speed that depends on the specific model of vehicle j and the conditions of the road where it moves (let us remark that this approach allows us to consider vehicles in the same scenario that can behave according to different steering dynamics). This constraint abstracts the dynamic limitations of the vehicle while executing the evasive maneuver at high speeds (for a more in-depth explanation in this regard, see Section V). Hence

$$|a_j(t)| \leq c_j(v_I), \qquad t \in [0, t_f], \quad j \in \{1, \ldots, L\}. \qquad (2)$$

2) **Lateral position restrictions**. The vehicles can only have a lateral displacement inside the width limits of the road and their dimensions cannot overlap. Hence

$$0 < x_1(t) \pm \frac{w_1}{2} < \cdots < x_L(t) \pm \frac{w_L}{2} < W, \qquad t \in [0, t_f]. \qquad (3)$$

B. Performance Functional

The following key objectives of this MOP are summarized next:

1) $f_{x,m}$: Minimization of the sum of the square of vehicle–vehicle and vehicle–obstacle pair distances at the end of the computed trajectory (at t_f) for each possible heading combination m (see Fig. 3). This term is used for

each vehicle to maximize the lateral distances at the time instant the obstacles' longitudinal position is reached.

2) f_v: Minimization of the sum of the square of the lateral speeds at the end of the trajectory (at t_f). The purpose of this term is to reduce the lateral speed at the time instant the obstacle/s is/are reached.
3) f_a: Minimization of the sum of the square of accelerations along the trajectory (during the whole interval $[0, t_f]$). This term is used to reduce the negative impact on comfort of large lateral accelerations along the trajectory.

To characterize the optimization problem, the overall idea is to evaluate the functional of every possible combination of vehicles into gaps and select the combination with the lowest performance cost.

More formally, when a total of L vehicles is approaching $M+2$ obstacles, each vehicle has at most $M+1$ gaps to pass through (independently of the remaining space) and they cannot overlap each other laterally while executing the trajectories. Taking the two previous premises into account, the total number of compositions of vehicles through gaps is $R_{L,M+1} = \binom{M+L}{L}$ (see Fig. 3 for a given example), where $R_{L,M+1}$ corresponds to the number of solutions of the general *nonnegative-integer-sum equality* problem [26]. In this regard, let $G_{m,\beta}^{(L,M)}$ denote the number of vehicles willing to pass through a certain gap $\beta \in \{1, \dots, M+1\}$ in the combination $m \in \{1, \dots, R_{L,M+1}\}$. These numbers $G_{m,\beta}^{(L,M)}$ are obtained by solving

$$\sum_{\beta=1}^{M+1} G_{m,\beta}^{(L,M)} = L, \qquad 0 \leq G_{m,\beta}^{(L,M)} \leq L. \tag{4}$$

In addition, let $\Xi_{m,l}^{(L,M)} = \sum_{\beta=1}^{l} G_{m,\beta}^{(L,M)}$ denote the cumulative sum of vehicles until gap β. For notation ease, superindex $^{(L,M)}$ will be omitted in the following equations, assuming that these parameters, namely, L and M, are previously established and known. Since trajectories do not overlap, vehicles maintain their order in the x-axis, so that the indexes of the $G_{m,\beta}$ vehicles heading for gap β in the combination m will be $\{\Xi_{m,\beta-1}+1, \dots, \Xi_{m,\beta}\}$.

As we said, the general idea is to quantify mathematically how good it is for the $G_{m,\beta}$ vehicles leading to a certain gap β to pass through it, and do the same for the rest of the gaps of this combination m. This goodness is calculated by the $\phi_{m,\beta}(t)$ function, which will be defined later. Then, for a combination m, the results of the $\phi_{m,\beta}(t)$ function for the $M+1$ gaps ($\beta \in \{1, \dots, M+1\}$) are summed, giving the performance cost of the final lateral distances ($f_{m,x}$) as obtained by the corresponding trajectory headings in combination m. Adding the other two performance criteria f_v and f_a to the $f_{m,x}$ function of combination m will give us the total performance cost functional of vehicles choosing to pass through obstacles as defined by the ordering scheme of the present combination m. By doing this for the rest of the $R_{L,M+1}-1$ combinations, we will obtain the set of performance cost functionals $\{J_{L,M}^{(1)}, \dots, J_{L,M}^{(R_{L,M+1})}\}$ regarding all combinations. Then, we minimize each $J_{L,M}^{(q)}$ subfunctional to obtain the new set $\{\overline{J_{L,M}^{(1)}}, \dots, \overline{J_{L,M}^{(R_{L,M+1})}}\}$, from which we will choose the entry with the lowest value, namely, $\overline{J_{L,M}^{(q)}}$.

Let us now express the previous concepts more formally. For each $m \in \{1, \dots, R_{L,M+1}\}$, we solve the optimization problem

$$\begin{cases} \text{minimize} & J_{L,M}^{(m)} \\ \text{s.t.} & \text{constraints} \end{cases} \tag{5}$$

by using gradient descent with constraining relations [19], [27]. The result is a locally optimal value of the functional and its associated control history, namely, $\overline{J_{L,M}^{(m)}}$ and $\overline{a_j^{(m)}}(t)$, $t \in [0, t_f]$, respectively.

If we now formulate the general problem as

$$\begin{cases} \text{minimize} & J_{L,M} \\ \text{s.t.} & \text{constraints} \end{cases} \tag{6}$$

then, to solve (6), we have to choose the combination $q \in \{1, \dots, R_{L,M+1}\}$ with the lowest performance metric, that is

$$\overline{J_{L,M}} = \min\left\{\overline{J_{L,M}^{(1)}}, \dots, \overline{J_{L,M}^{(R_{L,M+1})}}\right\} = \overline{J_{L,M}^{(q)}}. \tag{7}$$

Therefore, the control history values that globally minimize the functional $J_{L,M}$ are those associated with this combination q, that is

$$\overline{a_j}(t) = \overline{a_j^{(q)}}(t), \qquad t \in [0, t_f]. \tag{8}$$

The $J_{L,M}^{(m)}$ functions take the weighted sum expression

$$J_{L,M}^{(m)} = \theta_x \hat{f}_{m,x} + \theta_v \hat{f}_v + \theta_a \hat{f}_a \tag{9}$$

where $\hat{f}_{m,x}$, $\hat{f}_v$, and $\hat{f}_a$ correspond to the utopia/nadir functional normalization of $f_{m,x}$, f_v, and f_a, respectively, and θ_x, θ_v, and θ_a represent the design factors of the weighted sum functional, with $0 \leq \{\theta_x, \theta_x, \theta_x\} \leq 1$ and $\theta_x + \theta_x + \theta_x = 1$ (convex combination of weights). The normalization of a generic functional f_i according to the utopia/nadir scheme is obtained by the expression $\hat{f}_i = (f_i - f_i^{\mathcal{U}})/(f_i^{\mathcal{N}} - f_i^{\mathcal{U}})$, where $f_i^{\mathcal{U}}$ and $f_i^{\mathcal{N}}$ correspond to the utopia and nadir points of the generic functional f_i, respectively (see reference [28]). Using this normalization scheme allows the three subfunctionals of (9) to contribute proportionally (each one takes values between 0 and 1) to the weighted aggregation sum, which clearly improves the convergence of the optimization method (see [29] for more details).

For each subfunctional, we have

$$\begin{cases} f_{m,x} = \sigma_{m,\text{dist}}^2(t_f) \\ f_v = \sum_{j=1}^{L} v_j^2(t_f) \\ f_a = \sum_{j=1}^{L} \int_0^{t_f} a_j^2(t)dt \end{cases} \tag{10}$$

where in this case $f_{m,x} = \sigma_{m,\text{dist}}^2(t_f)$ represents the sum of the squared distances of vehicles to the limits of each gap, in every combination and as explained earlier (f_v and f_a are obvious).

Continuing with $f_{m,x}$, we express $\sigma^2_{m,\text{dist}}(t)$ as

$$\sigma^2_{m,\text{dist}}(t) = \sum_{\beta=1}^{M+1} \phi_{m,\beta}(t) \tag{11}$$

with

$$\begin{aligned}\phi_{m,\beta}(t) = &(z_{\beta+1} - z_\beta - C_1)^2 \\ &+ G_{m,\beta}\Bigg[\left(x_{\Xi_{m,\beta-1}+1}(t) - z_\beta - C_2\right)^2 \\ &\quad + \left(z_{\beta+1} - x_{\Xi_{m,\beta}}(t) - C_3\right)^2 \\ &\quad - \frac{(z_{\beta+1} - z_\beta - C_1)^2}{G_{m,\beta}}\Bigg] \\ &+ \sum_{l=\Xi_{m,\beta-1}+1}^{\Xi_{m,\beta}-1}\Bigg[(x_{l+1}(t) - x_l(t) - C_4(l+1))^2 \\ &\quad - \left(x_{\Xi_{m,\beta-1}+1}(t) - z_\beta - C_2\right)^2 \\ &\quad - \left(z_{\beta+1} - x_{\Xi_{m,\beta}}(t) - C_3\right)^2\Bigg]\end{aligned} \tag{12}$$

where we have

$$C_1 = \frac{o_{\beta+1} + o_\beta}{2} \quad C_2 = \frac{w_{\Xi_{m,\beta-1}+1} + o_\beta}{2}$$
$$C_3 = \frac{o_{\beta+1} + w_{\Xi_{m,\beta}}}{2} \quad C_4(l) = \frac{(w_l + w_{l-1})}{2} \tag{13}$$
$$G_{m,0} = 0 \quad G_{m,M+2} = 0. \tag{14}$$

We see that the $\phi_{m,\beta}(t)$ function computes the squared distances between the vehicular projections and the limits imposed by the βth gap (z_β and $z_{\beta+1}$) of the the mth combination. Finally, (11) calculates the sum of the local squared distances $\phi_{m,\beta}(t)$ of the $M+1$ gaps in combination m, giving the total cost of the L vehicles overcoming the obstacles as determined by composition m.

The following step is to obtain the acceleration history $a_j(t)$ for the L vehicles, which minimizes the $J^{(m)}_{L,M}$ function for each instance of the $R_{L,M+1}$ possible combinations during the maneuverability time interval $[0, t_f]$, and then choose the one that minimizes the problem (6). In order to do this, we make use of a gradient-descent–based approach, for which we 1) discretize the acceleration history of each of the L vehicles into N time instants $a_j(k), k \in \{0, \ldots, N\}$, 2) express the functionals $J^{(m)}_{L,M}$ in terms of this discretized control history, and 3) derive with respect to a fixed $a_p(s)$[6] ($1 \le p \le L, 0 \le s \le N$) to carry out the gradient descent.

[6]To obtain the derivatives of $J^{(m)}_{L,M}$ w.r.t. $a_j(k)$, we must first formulate the discretized expressions of $x_j(t)$ and $v_j(t)$ in terms of the control history $a_j(k)$: from the state equations in (1), we get $x_j(k+1) = X_{0j} + (k+1)\Delta t \cdot V_{0j} + (\Delta t)^2 \cdot \sum_{l=0}^{k-1}(k-l)\cdot a_j(l)$ and $v_j(k+1) = V_{0j} + \Delta t \cdot A_{0j} + \Delta t \cdot \sum_{l=1}^{k} a_j(l)$, respectively. Δt corresponds to the discretized time lapse resulting from the fraction between the maneuverability time interval t_f and the discretization factor N.

The discretized version of the $J^{(m)}_{L,M}$ function takes the form

$$\begin{aligned}J^{(m)}_{L,M} = &\theta_x\left[\frac{\sigma^2_{m,\text{dist}}(N) - \sigma^{2(\mathcal{U})}_{m,\text{dist}}(N)}{\sigma^{2(\mathcal{N})}_{m,\text{dist}}(N) - \sigma^{2(\mathcal{U})}_{m,\text{dist}}(N)}\right] \\ &+ \theta_v\left[\frac{\sum_{j=1}^{L} v_j^2(N) - \sum_{j=1}^{L} v_j^{2(\mathcal{U})}(N)}{\sum_{j=1}^{L} v_j^{2(\mathcal{N})}(N) - \sum_{j=1}^{L} v_j^{2(\mathcal{U})(N)}}\right] \\ &+ \theta_a\left[\frac{\sum_{j=1}^{L}\sum_{k=0}^{N} a_j^2(k) - \sum_{j=1}^{L}\sum_{k=0}^{N} a_j^{2(\mathcal{U})}(k)}{\sum_{j=1}^{L}\sum_{k=0}^{N} a_j^{2(\mathcal{N})}(k) - \sum_{j=1}^{L}\sum_{k=0}^{N} a_j^{2(\mathcal{U})(k)}}\right]\end{aligned} \tag{15}$$

where we have used normalization as indicated earlier. Now we calculate the derivative of $J^{(m)}_{L,M}$ with respect to a fixed $a_p(s)$. Since the utopia and nadir points of each subfunctional [$(\cdot)^{(\mathcal{U})}$ and $(\cdot)^{(\mathcal{N})}$, respectively] are constant, we obtain

$$\frac{\partial J^{(m)}_{L,M}}{\partial a_p(s)} = \theta'_x\left(\frac{\partial \sigma^2_{m,\text{dist}}(N)}{\partial a_p(s)}\right) + \theta'_v\alpha_v(p,s) + \theta'_a\alpha_a(p,s) \tag{16}$$

with

$$\theta'_x = \frac{\theta_x}{\sigma^{2(\mathcal{N})}_{m,\text{dist}}(N) - \sigma^{2(\mathcal{U})}_{m,\text{dist}}(N)} \tag{17}$$

$$\theta'_v = \frac{\theta_v}{\sum_{j=1}^{L} v_j^{2(\mathcal{N})}(N) - \sum_{j=1}^{L} v_j^{2(\mathcal{U})}(N)} \tag{18}$$

$$\theta'_a = \frac{\theta_a}{\sum_{j=1}^{L}\sum_{k=0}^{N} a_j^{2(\mathcal{N})}(k) - \sum_{j=1}^{L}\sum_{k=0}^{N} a_j^{2(\mathcal{U})}(k)}. \tag{19}$$

For the second and third terms of (16), we have

$$\alpha_v(n,l) = \begin{cases} 0 & n \neq p \\ 2\Delta t\left[V_{0p} + \Delta t A_{0p} + \Delta t \sum_{k=1}^{N-1} a_p(k)\right] & n = p \end{cases} \tag{20}$$

$$\alpha_a(n,l) = \begin{cases} 0 & n \neq p \vee l \neq s \\ 2\Delta t a_p(s) & n = p \wedge l = s. \end{cases} \tag{21}$$

If we focus now on the term in (16) containing $\sigma^2_{m,\text{dist}}$, we can define $\partial\sigma^2_{m,\text{dist}}(k)/\partial a_p(s)$ as

$$\frac{\partial \sigma^2_{m,\text{dist}}(k)}{\partial a_p(s)} = \begin{cases} \frac{\partial \phi_{m,\beta}(k)}{\partial a_p(s)} & \Xi_{m,\beta-1} + 1 \le p \le \Xi_{m,\beta} \\ 0 & \Xi_{m,\beta-1} + 1 > p \vee \Xi_{m,\beta} < p. \end{cases} \tag{22}$$

The condition in (22) for $\partial\sigma^2_{m,\text{dist}}(k)/\partial a_p(s) = 0$ is obvious (the derivative is not null only for those cases in which the

vehicle p is inside gap β); hence, we will focus only on the case where $\Xi_{m,\beta-1}+1 \leq p \leq \Xi_{m,\beta}$. From this we get

$$\begin{aligned}\frac{\partial \phi_{m,\beta}(k)}{\partial a_p(s)} &= G_{m,\beta}\left[2\left(x_{\Xi_{m,\beta-1}+1}(k)-z_\beta-C_2\right)\frac{\partial x_{\Xi_{m,\beta-1}+1}(k)}{\partial a_p(s)}\right.\\ &\quad\left.-2\left(z_{\beta+1}-x_{\Xi_{m,\beta}}(k)-C_3\right)\frac{\partial x_{\Xi_{m,\beta}}(k)}{\partial a_p(s)}\right]\\ &\quad+\sum_{m=\Xi_{m,\beta-1}+1}^{\Xi_{m,\beta}-1}\left[2\left(x_{m+1}(k)-x_m(k)-C_4(m+1)\right)\right.\\ &\quad\cdot\left(\frac{\partial x_{m+1}(k)}{\partial a_p(s)}-\frac{\partial x_m(k)}{\partial a_p(s)}\right)\\ &\quad-2\left(x_{\Xi_{m,\beta-1}+1}(k)-z_\beta-C_2\right)\\ &\quad\times\frac{\partial x_{\Xi_{m,\beta-1}+1}(k)}{\partial a_p(s)}\\ &\quad+2\left(z_{\beta+1}-x_{\Xi_{m,\beta}}(k)-C_3\right)\\ &\quad\left.\times\frac{\partial x_{\Xi_{m,\beta}}(k)}{\partial a_p(s)}\right]\end{aligned} \tag{23}$$

where

$$\frac{\partial x_j(k)}{\partial a_p(s)}=\begin{cases}0 & (p\neq j)\vee(k<s+2)\\ (\Delta t)^2(k-s-1) & (p=j)\wedge(k\geq s+2)\end{cases}. \tag{24}$$

It is possible to particularize (23) further depending on the surrounding elements of the derivation index p, by abstracting position, speed, acceleration, and width for vehicles and obstacles, as seen in

$$\begin{aligned}\frac{\partial \phi_{m,\beta}(k)}{\partial a_p(s)} &= 2(\Delta t)^2(k-s-1)\\ &\quad\times\left[(2\pi_{0p}-\pi_{0p+1}-\pi_{0p-1})\right.\\ &\quad+k\Delta t(2\lambda_{0p}-\lambda_{0p+1}-\lambda_{0p-1})\\ &\quad+\frac{\varpi_{p+1}-\varpi_{p-1}}{2}+(\Delta t)^2\sum_{l=0}^{k-2}(k-l-1)\\ &\quad\left.\times(2\psi_p(l)-\psi_{p+1}(l)-\psi_{p-1}(l))\right]\end{aligned} \tag{25}$$

where

$$\begin{cases}\left.\begin{matrix}\psi_n(l)=0\\ \lambda_{0n}=0\\ \pi_{0n}=z_{\beta-1}\\ \varpi_n=o_{\beta-1}\end{matrix}\right\} & n\leq\Xi_{m,\beta-1}\\ \left.\begin{matrix}\psi_n(l)=a_n(l)\\ \lambda_{0n}=V_{0n}\\ \pi_{0n}=X_{0n}\\ \varpi_n=w_n\end{matrix}\right\} & \Xi_{m,\beta-1}<n<\Xi_{m,\beta}+1\\ \left.\begin{matrix}\psi_n(l)=0\\ \lambda_{0n}=0\\ \pi_{0n}=z_\beta\\ \varpi_n=o_\beta\end{matrix}\right\} & n\geq\Xi_{m,\beta}+1.\end{cases} \tag{26}$$

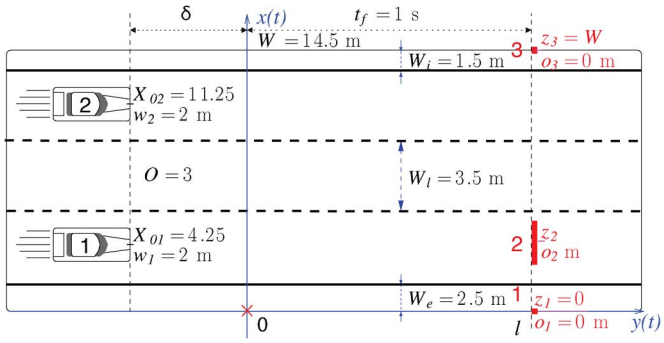

Fig. 4. Particular scenario used for evaluation.

Equation (25) and its particularization in (26) reflect the influence on the mobility of vehicle p (term ψ_p) due to its immediate neighbors (terms ψ_{p+1} and ψ_{p-1}), depending on the class of element (either if both are obstacles, one vehicle and one obstacle, or two vehicles).

IV. Evaluation Results

Here, we characterize the trajectory generation algorithm for a specific scenario by assessing:

- The effect of different values of the discretization factor N on the processing time of the preview trajectories [see Fig. 5(a) and (b)].
- The influence of the different components of the functional on the preview trajectories and the simulation results regarding the path-tracking process of these trajectories for a specific vehicle model [see Fig. 6(a)–(d)].

In particular, we focus on the analysis of the scenario shown in Fig. 4, where $L=2$ vehicles circulate at $v_I=33$ m/s (120 km/h). At $t=-\delta$ s, both vehicles discover $M+2=3$ obstacles ($M=1$ central object and the 2 default crash barriers) on the road $\delta\cdot v_I+l$ meters ahead, needing δ s to compute and negotiate the cooperative evasive scheme and using the remaining t_f s to execute the associated maneuvers. We will consider that δ corresponds to the optimization time interval of the $J_{L,M}^{(m)}$ combination with the largest duration among the set of $R_{L,M+1}$ combinations (we assume that all $J_{L,M}^{(m)}$ combinations are optimized in parallel).

The negotiation scheme is assumed to be instantaneous (in this paper, we focus exclusively on the proposed trajectory generation method), and the utopia/nadir normalization is performed offline; hence, both processes do not compute for the δ interval. The value of the maximum allowable lateral acceleration that vehicles can reach is taken from [35] ($c_j(v_I)=5.5432$ m/s^2), using the regression model in [35] for $\Gamma'=9.42$ m/s^2 and $\Delta C'=3.56$ km^{-1} (*fast driving* conditions). These values are based on an average estimation of the extreme steering capabilities extracted from multiple test-benches of a Renault Laguna on a Renault test track in France (see [35]). As explained in Section III-A, it is possible to set different values for this constraint on the maximum lateral acceleration, depending on the specific model involved. In this case, however, we will simulate a scenario with two vehicles subject to the same steering dynamics. As regards the path-tracking process,

TABLE I
CONFIGURATION SETUP FOR THE PATH-TRACKING SIMULATION

Vehicle configuration	
Parameter	**Value**
Sprung mass	C-Class Hatchback Sprung Mass 2012
Aerodynamics	C-Class, Hatchback Aero
Powertrain	FW drive 125 kW, 6-spd., 4.1 R. w/ Visc. Diff.
Steering system	C-Class, Hatchback: Power, R&P
Front/rear kinematics	C-Class, Hatchback
Front/rear compliance	C-Class, Hatchback
Tires	215/55 R17
Procedure	
Parameter	**Value**
Initial Speed	120 km/h
Braking control	No braking
Shifting control	AT 6th Mode
Steering: path-follower	Preview time: constant Driver preview time: 0.25 s Driver time lag: 0 s Funcion type: Spline Interp. & Extrap.
Start time	0 s
Stop time	1 s
Start (path station)	0 m
Stop (path station)	33 m

we will simulate the procedure "Steering: Driver path follower" with a constant speed in the direction of transit of 120 km/h, without braking, and for the "C-Class, Hatchback" vehicle model [7]. Preview trajectories obtained by our algorithm will be coupled in the path-tracking simulation platform, by using a constant driver preview time of 0.25 s and a time lag of 0 s. For more details on the configuration setup, see Table I (more information in [7]).

For the road dimensions, we choose the corresponding values found in [36], where there are three lanes, each 3.5 m wide, with external and internal edge measuring 2.5 and 1.5 m, respectively. Design parameters $\theta = [\theta_x, \theta_v, \theta_a]$ are normalized to accept values between 0 and 1: the closer each factor is to 1, the higher will be the influence of its corresponding functional on the weighted aggregation.

Fig. 5(a) and (b) illustrates the generated trajectories and the discretization points for which the previewed exact positions of the vehicles are calculated. Fig. 6(a)–(d) shows the preview trajectories (such as Fig. 5, in red without the discretization points) and the corresponding tracked paths according to the path-following execution in the simulator CarSim [7]. These tracked paths are represented at different time instants during the maneuver, with the exact position and orientation of the vehicle (in rectangular form), the vertical forces acting on each wheel (represented by circles on each corner of the rectangles), and the speed vectors indicating the lateral speed at each represented instant. Circles reflect the vertical load transference to each wheel of the vehicle with an area that depends on the radius, calculated by normalizing the corresponding vertical load with a value[7] of 6000 N: the bigger the area, the greater will be the supported vertical load by the corresponding wheel.

The cooperative evasive action covers the time interval $t \in [-\delta, t_f]$, since vehicles detect the obstacles ($t = -\delta$ s) until they reach their longitudinal position ($t = t_f$ s). Apart from this, vectors representing lateral speeds, which emerge from each represented picture in the graph, will provide additional information on the inertial behavior [the lateral speed $v_j(t)$] of the vehicle along the tracked maneuver. Obstacles are printed as red lines and, lanes and external/internal edges are delimited in graphs by corresponding gray (dashed) lines when applicable. The software MATLAB (version 7.10.0, R2010a) is used to perform all the mathematical calculations in a Windows 7 64-bit platform, with Intel(R)-Core 2 Duo CPU at 2 GHz, and 4-GB RAM.

[7]Normalizing respect to this value is due to the fact that the vertical loads of each wheel take half this quantity on average, in this way helping for visualization purposes.

A. *Influence of the Discretization Factor N*

The two graphs in Fig. 5 show the generated trajectories for the scenario depicted in Fig. 4, according to two different values of the discretization factor N, that is, two different levels of resolution, which consequently produce different computation overheads (δ s). As expected, in Fig. 5(b), the trajectory generation process takes a longer duration ($\delta = 0.3$ s) to be completed than the case in Fig. 5(a) ($\delta = 0.1$ s). The only wide-enough gap through which vehicles can simultaneously circulate can be found on the upper side of the road. From these results, we can clearly notice how important it is in this particular algorithm to reach a tradeoff between the accuracy of the computed trajectory and the delay for its calculation. Since trajectories must be generated with minimum delays, this is actually a critical issue.

B. *Trajectory Shaping Influence and Mechanical Response*

Graphs in Fig. 6 show the generated trajectories (in red) and the tracked paths by means of simulation for different configurations of the weighting factors $\{\theta_x, \theta_v, \theta_a\}$, in a slightly different scenario, where the central obstacle has different dimensions, leaving two wide-enough gaps on both sides. Prioritizing only on the minimization of the squared sum of lateral distances ($\theta_x = 1$), it is shown in Fig. 6(a) that both vehicles turn, in this case, their directions of movement toward the upper gap, which is clearly wider than the lower gap. Analyzing the dynamics of the maneuver, we find out that vehicle 1 executes a harder turn when compared to that of vehicle 2, as can be inferred from the evolution of its lateral speed and the big load transference toward the front right wheel.

In Fig. 6(b), we set the weighting factor θ_v to have influence on the generated trajectory ($\theta_x = 0.9, \theta_v = 0.1$). This time, vehicle 1 selects the lower gap to pass through, in order to minimize lateral speed at the end of the path while simultaneously minimizing the sum of squared lateral distances (choosing the upper gap would incur into a collision with this configuration of weights). However, in this case, the load transference oscillates from the left to the right wheels during the maneuver, increasing the risk of losing control of the vehicle due to a decrease in the stability of the car body.

On the other hand, in Fig. 6(a) and (d), we show the generated trajectories when influenced by the third term in the functional ($\theta_a = 0.05$). We observe in those cases the lower rate of change of lateral speed during the maneuver (as seen

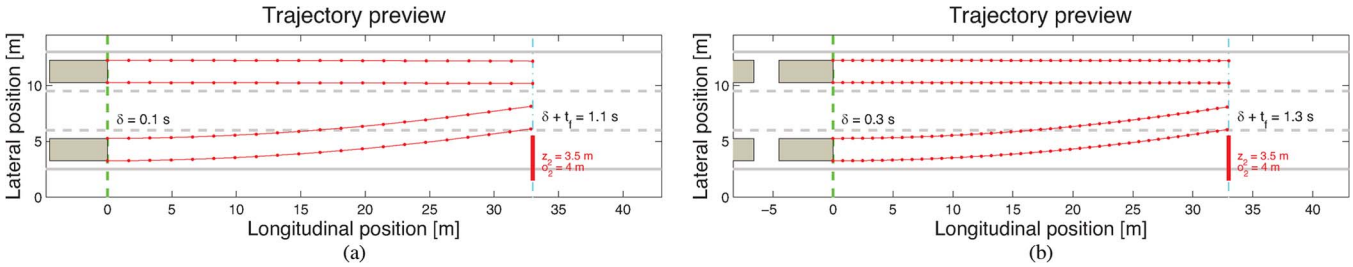

Fig. 5. Preview evasive maneuvers for different discretization factors: $N = 20$ and $N = 40$. (a) $N = 20$, $L = 2$ vehicles, $M = 1$ obstacle. (b) $N = 40$, $L = 2$ vehicles, $M = 1$ obstacle.

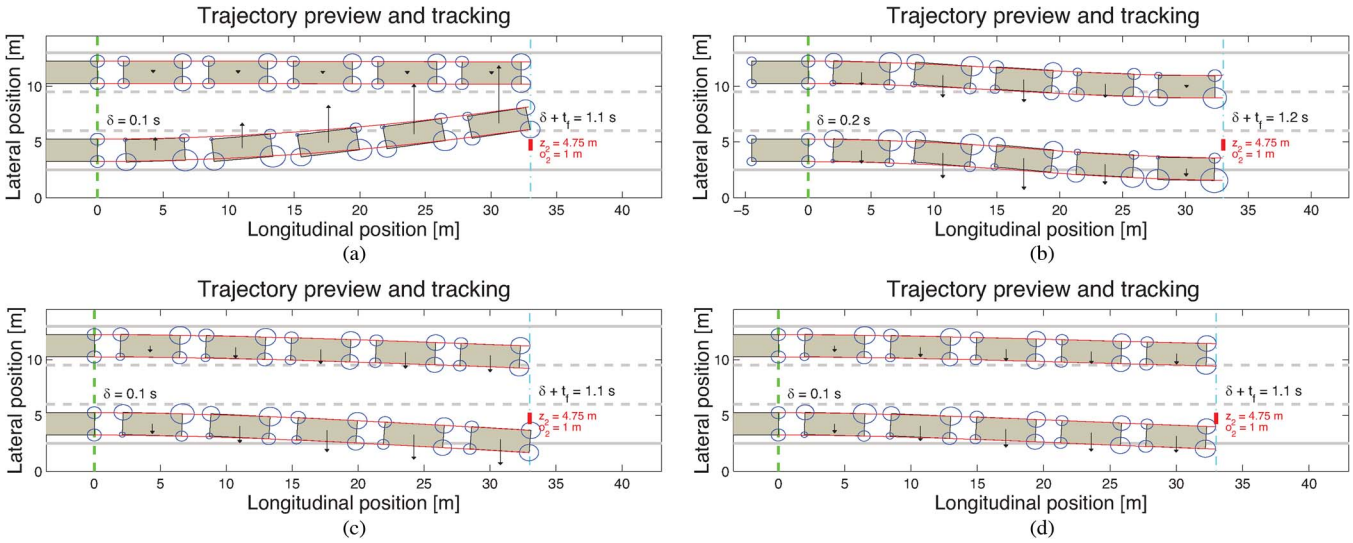

Fig. 6. Preview evasive maneuvers and path-tracking results (vehicular positions at different time instants during the maneuvers) for different configurations of the weighting factors. (a) $\{\theta_x, \theta_v, \theta_a\} = \{1, 0, 0\}$, $L = 2$ vehicles, $M = 1$ obstacle. (b) $\{\theta_x, \theta_v, \theta_a\} = \{0.9, 0.1, 0\}$, $L = 2$ vehicles, $M = 1$ obstacle. (c) $\{\theta_x, \theta_v, \theta_a\} = \{0.95, 0, 0.05\}$, $L = 2$ vehicles, $M = 1$ obstacle. (d) $\{\theta_x, \theta_v, \theta_a\} = \{0.9, 0.05, 0.05\}$, $L = 2$ vehicles, $M = 1$ obstacle.

from the velocity vectors), with a lower final lateral speed in Fig. 6(d) in comparison with Fig. 6(c), as entailed from setting $\theta_v = 0.05$ in Fig. 6(d). In these cases, it is easy to notice how the load transference between axes has been smoothed, producing maneuvers that, despite not leading to the same results in Fig. 6(a) and (d) (in terms of maximization of the lateral distance and/or minimization of the final lateral speed), turn out to provide better stability of the car body during the path-tracking process.

V. Discussions on the Model

In the following subsections, we explain in detail important key aspects over the model and the results obtained. First, we focus on the flexibility of the proposal to shape trajectories according to the needs of the decision-maker. Second, a discussion on the convergence times that the proposal needs to compute the evasive trajectories is presented. Third, we convey some important comments on the sensitivity of the model to the given dynamic assumptions. Last, but not least, some ideas over a potential communications' protocol that implements the agreement phase are introduced.

A. Trajectory Shaping

We can see from the previous results how we can adjust the shape of trajectories by appropriately setting the values of the weights of the aggregated sum functional. Since the weights determine the safety and comfort results of the MOP, a thorough evaluation of their effects under a wide number of situations is required, in order to design an application that actively chooses the best policy according to the specific traffic situation in which vehicles are involved. Along with this evaluation, it is important to conduct an additional comparison with other related approaches (elastic bands, tree search, etc.) to test different important aspects of the algorithm that are out of the scope of this paper. This is left as future work.

B. Convergence Time of the Algorithm

In Fig. 5(a) and (b), we observed that the time taken to process the trajectories tightly depends on the discretization factor N, as expected. A rigorous algorithm convergence study requires a future work; at the moment, we include a brief evaluation of the algorithm convergence time for two particular scenarios, for different values of the θ_v and θ_a parameters ($\theta_x = 1 - \theta_v - \theta_a$). Fig. 7(a) represents a 3-D bar chart containing the 10-run averaged computation times (δ) for the represented values of the θ_v and θ_a design factors ($\theta_x \geq 0.8$), in the same scenario as the one depicted in Fig. 4 ($L = 2$ vehicles, $M = 1$ intermediate obstacle). Fig. 7(b) represents the same scenario with $L = 3$ vehicles and $M = 1$ intermediate obstacle. Without optimization techniques to reduce this computation time, we can obtain acceptable processing delays (δ) for the purpose

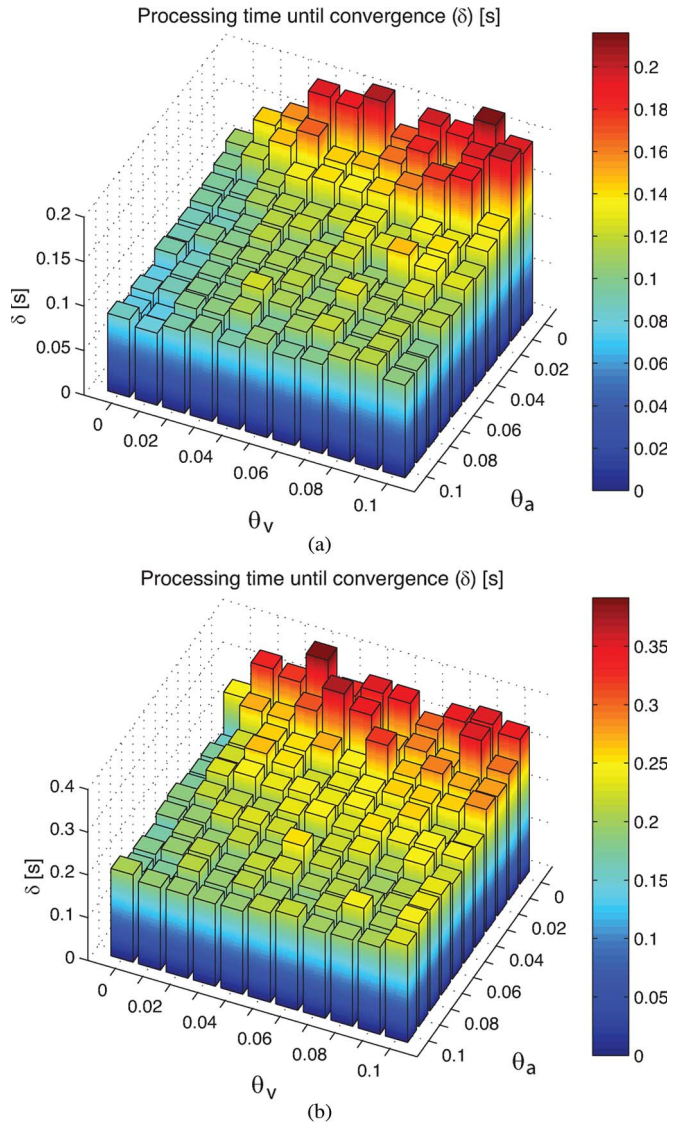

Fig. 7. Averaged convergence times for two scenarios. (a) $L = 2$ vehicles, $M = 1$ intermediate obstacle. (b) $L = 3$ vehicles, $M = 1$ intermediate obstacle.

of a safety application [$\sim$100 ms in Fig. 7(a) and $\sim$200 ms in Fig. 7(b)]. From both figures, we notice that higher values of the θ_a parameter result in shorter computation times δ because since the initial guess for the gradient descent is set to $a_j(k) = 0, j \in \{1, \ldots, L\}, k \in \{0, \ldots, N\}$ and θ_a shapes the influence on the minimization of accelerations along the maneuver [subfunctional f_a in (10)], the number of iterations until converging to the solution is lower than for smaller values of θ_a. Although not directly suitable for real-time applicability, these results give us an optimistic hint on the potential use of this procedure for practical applications. The authors plan to use more powerful equipment for the calculation process, as well as carry out a software optimization of our proposal to accelerate the trajectory calculation procedure. Another option might be to use more efficient optimization solvers that can increase computation speed, such as CPLEX [31] or GLPK [32]. Some other approaches, such as evolutionary optimization [34] or heuristic optimization [34], can be analyzed and compared to test the performance of the algorithm in a more objective context.

C. Sensitivity of the Model

According to the particular characteristics of the scenario under study, we assume a constant longitudinal speed v_I (refer to the Appendix), as well as the particular situation in which vehicles are located in the same longitudinal position (and thus, fixed maneuverability time interval t_f). Despite not being very realistic considerations, these are justified by the fact that, when vehicles circulating in parallel must turn at very high speeds, it is much easier to control the lateral mobility, rather than the longitudinal movement. Therefore, we can focus exclusively on handling the lateral displacement to avoid the potential collisions. Additionally, using brakes might also transfer the vertical loads to the front wheels, thus reducing the potential maneuverability of the vehicle to avoid the collisions.

On the other hand, as was introduced in Section IV, we consider the dynamic constraints to be abstracted by the maximum allowable lateral acceleration value, as obtained by the experiment given by Reymond *et al.* [35]. The authors in [35] explicitly state that it is possible to map angular (in our case, represented by the steering angle $\gamma_j(t)$) and linear mobility (speed in the direction of movement v_I) from the vehicle model to actuator commands that serve to handle the corresponding tilt and roll car dynamics. As these authors also justify in [35], there already exist so-called tilt coordination algorithms that are used to scale the given angular/linear accelerations to the specific tilt/roll dynamic actuators of the car, considering weight, surface traction condition of wheels with the road, etc. Of course, this mapping operation depends on the specific mechanic/dynamic properties of the vehicle under motion and the conditions where it moves (dry surface, rain, etc.).

However, it is important to carry out an extensive analysis on the sensitivity of this proposal, in order to quantify more exhaustively the validity of the given dynamic assumptions of the model. One of the short-term objectives is to carry out this additional analysis to guarantee a certain number of conditions under which generated trajectories are feasible in a real context.

D. Protocol for Trajectory Set Agreement

In addition, we considered that the negotiation process was instantaneous, thus not computing for the δ interval. In practice, such assumption should not be neglected, because the cooperative agreement of vehicles on the trajectories to follow might work according to a certain scheme that might slightly delay the moment at which the maneuvers begin. Other aspects such as timing synchronization or sharing the communication's channel with other background traffic that might affect performance could be relatively important. Thus, it is relevant to conduct a more in-depth study of a communication protocol supported by the already existing Wireless Access in Vehicular Environments Standard (WAVE) architecture [30] that takes these issues into close consideration.

VI. Conclusion

This paper presents an algorithm to calculate optimum evasive trajectories for a generic number of vehicles and obstacles.

Specifically targeted for extreme situations in which high-speed vehicles need to take such maneuvers, the main characteristics of the algorithm are the following:

- It generates evasive trajectories subject to time constraints, for an arbitrary number of vehicles and obstacles to circumvent.
- It provides ample flexibility to adjust the shape of the trajectories by handling additional aspects, such as the final lateral speed and the lateral inertia along the path.
- The initial evaluation of the algorithm convergence times, without specific performance optimization, shows that it can be applied in a practical scenario.

The dynamic behavior of the vehicles while tracking the calculated trajectories has been also simulated for a better understanding of the mechanical aspects associated to the given emergency maneuvers.

APPENDIX A
JUSTIFICATION OF MODEL ASSUMPTIONS

Given that we assume constant longitudinal speed v_I m/s and that we only handle lateral mobility to determine the evasive trajectories, it is important to quantify the Euclidean distance error between 1) the hypothetical trajectory that would be tracked by a nonrotating vehicle, which would displace laterally (according to the computed lateral accelerations) with a fixed longitudinal speed v_I m/s, and 2) the generated trajectory that is calculated for a rotating vehicle whose speed in the direction of movement is set to v_I m/s and its steering angle is obtained according to the expression $\gamma_j(t) = \arcsin(v_j(t)/v_I)$. This mapping operation is necessary because, in practice, what we need to update the trajectory of a vehicle is, in the simplest sense, the steering angle $\gamma_j(t)$ and the speed in the direction of movement. The main reason for the initial constant-longitudinal-speed assumption was to have a fixed maneuverability interval t_f to keep the integral limits of the performance costs in (6) constant also. This assumption considerably reduces the complexity of the problem because we integrate functionals for a fixed interval of time $[0, t_f]$ s, at the expense of increasing the associated longitudinal error of the mapped trajectories for decreasing values of the longitudinal speed (higher lateral accelerations).

Examining first Fig. 8(a), we see a contour representation of the longitudinal distance error of the mapped trajectory for the extreme situation, in which a vehicle executes its maneuver by using the maximum allowable acceleration (represented in the horizontal axis, namely, $c_j(v_I)$), against the maneuverability time interval t_f (subdividing the vertical axis). The representation shows the percentage of error with respect to the width of the vehicle (w_j). For example, if $w_j = 2$ m and the distance error is 10%, it means that the maximum longitudinal error at the end of the mapped trajectory is $\epsilon = 20$ cm. Assuming that lateral mobility keeps unchanged in the mapping process (the longitudinal speed is the only affected), we notice in Fig. 8(b) that the maximum error in the longitudinal distance increases with lower values of the longitudinal speed (v_I), due to the higher values of maximum lateral acceleration that vehicles can take while maneuvering at these speeds.

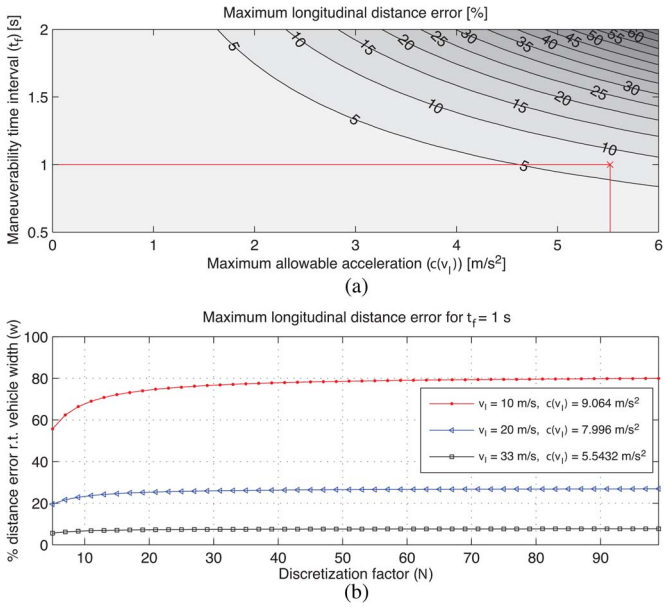

Fig. 8. Analysis of maximum longitudinal error for mapped trajectories. (a) Maximum deviation of mapped trajectories at the end of the time horizon (% w.r.t. w_j) for $N = 20$. (b) Evolution of maximum longitudinal distance error according to the discretization factor N.

In the case of this study, we carry out the trajectory generation procedure by assuming a $t_f = 1$ s and a maximum allowable lateral acceleration given by $c_j(v_I) = 5.5432$ m/s^2 (longitudinal speed of $v_I = 33$ m/s) that will reach a maximum longitudinal error of 7.7% with respect to the vehicle's width $(w_j = 2$ m), meaning a maximum of 15 cm of longitudinal error, quite reasonable indeed to keep a fixed t_f for the trajectory generation procedure.

ACKNOWLEDGMENT

The authors would like to thank C. Garcia-Costa for her suggestions that improved the text.

REFERENCES

[1] H. Hartenstein and K. Laberteaux, *VANET—Vehicular Applications and Inter-Networking Technologies*. Hoboken, NJ, USA: Wiley, 2010, pp. 219–272.
[2] T. L. Willke, P. Tientrakool, and N. F. Maxemchuk, "A survey of inter-vehicle communication protocols and their applications," *IEEE Commun. Surveys Tuts.*, vol. 11, no. 2, pp. 3–20, 2nd Quart., 2009.
[3] C. Frese, T. Batz, and J. Beyerer, "Cooperative behavior of groups of cognitive automobiles based on a common relevant picture," *Automatisierungstechnik*, vol. 56, no. 12, pp. 644–652, Dec. 2008.
[4] M. T. Wolf and J. W. Burdick, "Artificial potential functions for high-way driving with collision avoidance," in *Proc. IEEE ICRA*, May 2008, pp. 3731–3736.
[5] R. Lachner, M. H. Breitner, and H. J. Pesch, "Real-time collision avoidance: Differential game, numerical solutions, and synthesis of strategies," in *Annals-International Society of Dynamic Games*. New York, NY, USA: Springer-Verlag, 2000, pp. 115–136.
[6] C. Garcia-Costa, E. Egea-Lopez, J. B. Tomas-Gabarron, J. Garcia-Haro, and Z. J. Haas, "A stochastic model for chain collisions of vehicles equipped with vehicular communications," *Intelligent Transportation Systems, IEEE Transactions on*, vol. 13, no. 2, pp. 503–518, Jun. 2012.
[7] Mechanical Simulation Corporation. (2013, Feb.). CarSim mechanical simulation, Ann Arbor, MI, USA, Version 8.2.1. Trial License Number MLN23359. Retrieved 2013-06-13. [Online]. Available: http://www.carsim.com/products/carsim/index.php

[8] O. Khatib, "Real-time obstacle avoidance for manipulators and mobile robots," in *Proc. IEEE Int. Conf. Robot. Autom.*, Mar. 1985, vol. 2, pp. 500–505.
[9] T. Arai, H. Ogata, and T. Suzuki, "Collision avoidance among multiple robots using virtual impedance," in *Proc. IEEE/RSJ Int. Workshop IROS, Autonom. Mobile Robots Appl.*, Sep. 1989, pp. 479–485.
[10] S. Quinlan and K. Oussama, "Elastic bands: Connecting path planning and control," in *Proc. IEEE Int. Conf. Robotics Autom.*, 1993, pp. 802–807.
[11] S. K. Gehrig and F. J. Stein, "Elastic bands to enhance vehicle following," in *Proc. IEEE Int. Transp. Syst.*, 2001, pp. 597–602.
[12] T. Brandt, T. Sattel, and J. Wallaschek, "On automatic collision avoidance systems," in *Proc. SAE Int.*, 2005, pp. 316–326.
[13] O. Ararat and B. Aksun Guven, "Development of a collision avoidance algorithm using elastic band theory," in *Proc. 17th IFAC World Congr.*, Jul. 2008, pp. 6–11.
[14] C. Frese and J. Beyerer, "A comparison of motion planning algorithms for cooperative collision avoidance of multiple cognitive automobiles," in *Proc. IEEE IV Symp.*, Jun. 2011, pp. 1156–1162.
[15] S. Glaser, B. Vanholme, S. Mammar, D. Gruyer, and L. Nouveliere, "Maneuver-based trajectory planning for highly autonomous vehicles on real road with traffic and driver interaction," *IEEE Trans. Intell. Transp. Systems*, vol. 11, no. 3, pp. 589–606, Sep. 2010.
[16] L. Li and F. Y. Wang, "Cooperative driving at blind crossings using intervehicle communication," *IEEE Trans. Veh. Technol.*, vol. 55, no. 6, pp. 1712–1724, Nov. 2006.
[17] C. Frese, "Cooperative motion planning using branch and bound methods," in *Proc. Joint Workshop Fraunhofer IOSB Inst. Anthropom., Vis. Fusion Lab.*, 2010, pp. 187–201, KIT Scientific Publishing.
[18] C. Frese and J. Beyerer, "Planning cooperative motions of cognitive automobiles using tree search algorithms," in *Proc. KI 2010, Adv. Artif. Intell.*, 2010, pp. 91–98.
[19] D. E. Kirk, *Optimal Control Theory. An Introduction*. London, U.K.: Prentice-Hall, 1971, p. 453.
[20] A. Venkatraman and S. P. Bhat, "Optimal planar turns under acceleration constraints," in *Proc. 45th IEEE Conf. Decision Control*, Dec. 13–15, 2006, pp. 235–240.
[21] D. A. Anisi, J. Hamberg, and X. Hu, "Nearly time optimal paths for a ground vehicle," *J. Control Theory Appl.*, vol. 1, no. 1, pp. 2–8, Nov. 2003.
[22] T. Shamir, "How should an autonomous vehicle overtake a slower moving vehicle: Design and analysis of an optimal trajectory," *IEEE Trans. Autom. Control*, vol. 49, no. 4, pp. 607–610, Apr. 2004.
[23] J. B. Tomas Gabarron, E. Egea Lopez, and J. Garcia Haro, "Evaluating communications and intelligent driver model in a context of chain collision avoidance applications for VANETs," in *Proc. 3rd Int. Conf. RSS*, Indianapolis, IN, USA, Sep. 2011, pp. 13–15.
[24] D. N Godbole, V. Hagenmeyer, R. Sengupta, and D. Swaroop, "Design of emergency manoeuvres for automated highway systems: Obstacle avoidance problem," in *Proc. IEEE Conf. Decision Control*, 1997, pp. 4774–4779.
[25] P. Dingle and L. Guzzella, "Optimal emergency maneuvers on highways for passenger vehicles with two-and four-wheel active steering," in *Proc. ACC*, Jun. 30, 2010–Jul. 2, 2010, pp. 5374–5381.
[26] R. P. Stanley, *Enumerative Combinatorics*. Cambridge, U.K.: Cambridge Univ. Press, 2011, pp. 25–26.
[27] J. B. Rosen, "The gradient projection method for nonlinear programming. Part I. Linear constraints," *J. Soc. Ind. Appl. Math.*, vol. 8, no. 1, pp. 181–217, Mar. 1960.
[28] W. Stadler, *Multicriteria Optimization in Engineering and in the Sciences*. Berlin, Germany: Springer-Verlag, 1988.
[29] A. M. Jubril, "A nonlinear weights selection in weighted sum for convex multiobjective optimization," *Facta Univ. (NIS). Ser. Math. Informat.*, vol. 27, no. 3, pp. 357–372, 2012.
[30] *Wireless Access for Vehicular Environments Standard*, WAVE 1609/IEEE 802.11p, 2010.
[31] CPLEX. In Wikipedia, The Free Encyclopedia, Feb. 28, 2013, Retrieved 11:07 April 1, 2013. [Online]. Available: http://en.wikipedia.org/w/index.php?title=CPLEX
[32] GNU Linear Programming Kit. In Wikipedia, The Free Encyclopedia., Mar. 7, 2013, Retrieved 11:08, April 1, 2013. [Online]. Available: http://en.wikipedia.org/w/index.php?title=GNU_Linear_Programming_Kit
[33] E. Zitzler and L. Thiele, "Multiobjective optimization using evolutionary algorithms—A comparative case study," in *Parallel Problem Solving From Nature-PPSN V*. Berlin, Germany: Springer-Verlag, 1998, pp. 292–301.
[34] R. Storn and K. Price, "Differential evolution—A simple and efficient heuristic for global optimization over continuous spaces," *J. Glob. Optim.*, vol. 11, no. 4, pp. 341–359, Dec. 1997.
[35] G. Reymond, A. Kemeny, J. Droulez, and A. Berthoz, "Role of lateral acceleration in curve driving: Driver model and experiments on a real vehicle and a driving simulator," *Hum. Factors. J. Hum. Factors Ergonom. Soc.*, vol. 43, no. 3, pp. 483–495, Fall 2001.
[36] D. G. de Carreteras, "Centro de Publicaciones, Ministerio de Fomento," in *Trazado. Instrucción de Carreteras. Norma 3.1-IC*. Madrid, Spain: Publicación de Serie Normativas e Instrucción de Carreteras, 2011.

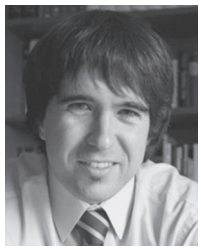

Juan-Bautista Tomas-Gabarron received the B.Sc. degree in telecommunications engineering and the Ph.D. degree in telecommunications from the Technical University of Cartagena (UPCT), Cartagena, Spain, in 2008 and 2013, respectively.

He is currently employed as a Ph.D. Researcher with UPCT. His research interests include vehicular ad-hoc networks, in particular the design, evaluation, and testing of cooperative collision avoidance applications for traffic safety enhancement.

Esteban Egea-Lopez received the B.Sc. degree in telecommunications engineering from the Polytechnic University of Valencia (UPV), Valencia, Spain, in 2000, the Master degree in electronics from the University of Gävle, Gävle, Sweden, in 2001, and the Ph.D. degree in telecommunications from the Technical University of Cartagena (UPCT), Cartagena, Spain, in 2006.

Since 2001, he has been an Assistant Professor with the Department of Information Technologies and Communications, UPCT. His research interest is focused on vehicular, ad-hoc, and wireless sensor networks and radio-frequency identification.

Joan Garcia-Haro (M'11) received the M.Sc. and Ph.D. degrees in telecommunication engineering from the Universitat Politecnica de Catalunya, Barcelona, Spain, in 1989 and 1995, respectively.

He is a Professor with the Technical University of Cartagena (UPCT), Cartagena, Spain. He is the author or coauthor of more than 70 journal papers, mainly in the fields of switching, wireless networking, and performance evaluation.

Dr. Garcia-Haro served as Editor-in-Chief of the IEEE Global Communications Newsletter from April 2002 to December 2004, included in the IEEE Communications Magazine, where he served as Technical Editor from March 2001 to December 2011. He also received an Honorable Mention for the IEEE Communications Society Best Tutorial Paper Award in 1995.